Quarkyonic percolation and deconfinement at finite density and number of colors

Stefano Lottini

ITP, J. W. Goethe Universität, Max-von-Laue-Straße 1, 60438 Frankfurt am Main, Germany

Giorgio Torrieri

FIAS, J. W. Goethe Universität, Ruth-Moufang-Straße 1, 60438 Frankfurt am Main, Germany and Pupin Physics Laboratory,
Columbia University, New York, New York 10027, USA

We examine the interplay between the percolation and the deconfinement phase transitions of Yang-Mills matter at finite temperature, quark chemical potential μ_Q, and number of colors N_c. We find that, whereas the critical N_c for percolation goes down with density, the critical N_c for confinement generally goes up. Because of this, Yang-Mills matter falls into two qualitatively different regimes: the "low-N_c limit," where percolation does not occur because matter deconfines before it percolates, and the "high-N_c limit," where there are three distinct phases—confined, deconfined, and confined but percolating matter—characterizing Yang-Mills matter at finite temperature and density. The latter can be thought of as the recently conjectured "quarkyonic phase." We attempt an estimate of the critical N_c to see if the percolating phase can occur in our world. We find that, while percolation will not occur at normal nuclear density as in the large-N_c limit, a sliver of the phase diagram in N_c, energy density and baryonic density where percolation occurs while confinement persists is possible. We conclude by speculating on the phenomenological properties of such percolating "quarkyonic" matter and suggesting avenues by which to study it quantitatively and to look for it in experiment.

I. INTRODUCTION: THE PHASE DIAGRAM AT LARGE N_c

The "large number of colors" approach [1,2] has been a promising way to simplify some of the tremendous mathematical difficulties inherent in handling nonperturbative features of Yang-Mills theory. The idea is to take the number of colors N_c to infinity while taking the Yang-Mills coupling constant g_{YM} to zero in such a way that $g_{\mathrm{YM}}^2 N_c = \lambda$ stays constant, defined at some perturbative fixed scale. Numerical results, obtainable by plugging in $N_c = 3$, should be correct within $\frac{1}{N_c} \sim 30\%$ or so, and hence this simplified theory should be enough for a qualitative estimate.

While this theory shares with QCD its nonperturbative nature (strong coupling arises at a scale $\sim N_c^0$, parametrically similar therefore to the QCD scale of $\Lambda_{\mathrm{QCD}} \simeq 250$ MeV), this approach has led to some important qualitative results: The fact that in a confined regime mesons are quasiparticles [1] while baryons are classical states [2] can be explained in this large-N_c limit. Features of QCD such as the dominance of planar diagrams (and hence the string description of gluon propagators and extension into the gauge/string correspondence [3]) and the OZI rule are also well explained with N_c counting. This has made large N_c a useful tool for phenomenological as well as theoretical analysis [4].

The large-N_c limit, however, has some qualitative differences from physical QCD, too, differences too big to be put down as a 30% correction.

Owing to the identification of confinement with center symmetry restoration [5–7], deconfinement is a first-order phase transition in the large-N_c limit provided that the number of light flavors $N_f \ll N_c$; it is a smooth crossover in our $N_c = 3$ world [8,9].

Nuclear matter is a tightly bound crystal in the large-N_c limit [10], whereas it is a liquid in our world [11–19]. The latter feature is a consequence of the fact that in the large-N_c limit the interbaryon binding energy scales as the baryon mass, $N_c \Lambda_{\mathrm{QCD}}$. In reality, the scale of internuclear forces is around $\sim \mathcal{O}[\Lambda_{\mathrm{QCD}}/(10\text{–}100)]$, a "hierarchy problem" which, given the soundness of the large-N_c description, needs to be resolved.

Given the considerations above, a *phase transition* in N_c, between $N_c = 3$ and $N_c \to \infty$, is a plausible resolution of some of these issues [20–22]. The existence of two possibly linked transitions in N_c is, in fact, fairly certain, owing to the arguments above: If we could keep N_f constant ($N_f \geqslant 1$ for baryons to exist) and increase N_c, we would find a critical point for confinement at zero quark chemical potential (somewhere between the crossover in our world and a first-order transition at $N_f/N_c \to 0$ [23,24]) and a liquid-crystal transition for matter at high chemical potential (because the large-N_c matter is crystalline [10] and a crystal-liquid transition is typically associated to a phase transition owing to a change in translational symmetries).

As discussed in Ref. [20] (and hinted at from gauge/string calculations [25,26]), the crystal-liquid transition is linked to the nuclear-matter hierarchy problem: The classical picture of the baryon necessarily entails an N_c much larger than $N_N \sim \mathcal{O}(10)$, where N_N is the number of neighbors in a densely packed system. Below this limit, one cannot ignore the Pauli exclusion principle in the *noncolor part* of the baryonic wave function. This raises the energy cost of compressing baryonic matter by $\sim N_c \Lambda_{\mathrm{QCD}}^3$ and hence most likely lowers the equilibrium density to values lower than $\sim \Lambda_{\mathrm{QCD}}^3$ (in fact, even $\ll m_\pi^3$). Because interquark interactions are suppressed by the confinement scale, and pionic exchanges are $\sim e^{-r m_\pi}$, the nuclear forces get weaker; hence, the critical point of the nuclear liquid-gas phase transition happens at $T, \mu_Q \ll \Lambda_{\mathrm{QCD}}$.

Going further is hampered by the fact that our understanding of corrections to N_c in this regime is limited. The regime in which this transition occurs is inevitably strongly coupled, making perturbative calculations untenable. Standard methods of lattice QCD cannot be used, because $\mu_Q/T \sim \mathcal{O}(1)$ [27–29]. As discussed in [30], gauge-gravity techniques are also unreliable because this transition, by its very nature, is *quantum-gravitational*, something of which we have a very limited understanding.

The only possible way to move forward, then, is to investigate models that are simple and qualitative, yet are universally applicable. One suggested way to describe phase transitions in Yang-Mills is via percolation [31–33]. The idea is that, at increasing energies, the increasing parton densities will make partons of different hadrons "overlap" as their interaction cross section becomes of the order of interparton spacing. It is logical to associate this transition to deconfinement, where a quark can propagate throughout the hot medium rather than being confined to the hadron size, whose natural scale is $\sim \Lambda_{\mathrm{QCD}}^{-1} \sim 1$ fm. While these analogies might touch on deeper conceptual issues [34], the percolation picture of confinement misses the order of the phase transition both at $N_c = 3$ and $N_c \to \infty$, so its direct relevance to confinement is questionable.

There is, however, a newly conjectured regime where the percolation picture might be viable: It is the proposed "quarkyonic matter" at low temperature (below the deconfinement temperature T_c) and moderate density (one baryon per baryonic size, $\mu_Q = \mu_B/N_c \simeq \Lambda_{\mathrm{QCD}}$) [35–41], which is confined (the excitations at the Fermi surface are baryonic) but "quarklike," in that pressure and perhaps also entropy density feel the quarks below the Fermi surface and consequently scale as N_c^1, as opposed to N_c^0.

Unlike in Refs. [31–33], the quarkyonic transition is thought to be *distinct* from deconfinement, to be found in lower energy heavy-ion scans [42–45] at low temperature but high baryochemical potential $\mu_B = N_c \mu_Q$ (a description of deconfinement at finite density as percolation was also postulated in Refs. [46,47]).

The reason for conjecturing the existence of a new phase boils down to comparing the quark-hole screening with the gluon-gluon antiscreening at large chemical potential (Fig. 1): Confinement is broken when the screening by quark-hole pairs $\sim \mu_Q^2 N_c N_f$ at the Fermi surface (which decreases the effective coupling) overpowers antiscreening by gluon loops ($\sim N_c^2$),

FIG. 1. (Color online) Panel (a) shows the interplay between antiscreening by gluons (driving confinement) and screening at high chemical potential. As the panel (b) shows, higher order corrections will not alter the dependence leading in N_f/N_c [48].
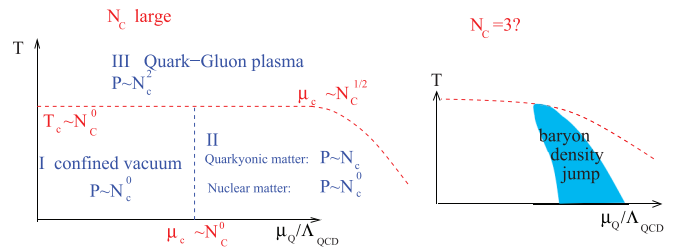
FIG. 2. (Color online) (Left) The phase diagram in the $N_c \to \infty$ limit, where the deconfinement line becomes flat as quark corrections vanish, and a first-order phase transition, with the baryon density as an order parameter, rises up vertically with respect to temperature at $\mu_Q \sim \Lambda_{\mathrm{QCD}}$. The scaling of the pressure with N_c is shown in the different phases. (Right) A qualitative sketch of the expected situation at $N_c = 3$.

which drives the coupling constant above nonperturbative values at momenta $\sim \Lambda_{\mathrm{QCD}}$ and ultimately causes the onset of the strong coupling regime. This can be used to get an estimate for the low-temperature deconfinement point as scaling *at least* as $\sim \Lambda_{\mathrm{QCD}} \sqrt{N_c/N_f}$. A cursory examination of Fig. 1 (bottom panel) shows that higher loops giving a $(N_c/N_f)^{z>1/2}$ scaling [48], and hence *perturbative* contributions to the QCD β function, cannot lower the extra scale $\mu_q \sim \sqrt{N_c/N_f}^{z \geqslant 1/2} \Lambda_{\mathrm{QCD}}$, which appears when one explores the deconfinement phase transition in chemical potential rather than temperature.

Thus, the phase diagram at $N_c \to \infty$ looks like the one in Fig. 2 (left) [35]: The deconfinement line becomes infinitely flat. At the same time, the transition to "nuclear matter," with the baryonic density as order parameter, becomes infinitely sharp because the baryon mass $\sim N_c \Lambda_{\mathrm{QCD}}$. Therefore, baryons drop out of the confined vacuum partition function entirely, but continue to be present at $\mu_Q \geqslant \Lambda_{\mathrm{QCD}}$.

Hence, nuclear matter at $\mu_Q \sim \Lambda_{\mathrm{QCD}}$ should, at large N_c, be in the confined phase. In configuration space, however, interquark distance $\sim N_c^{-1/3}$: For large-enough N_c, then, one should be in the confinement regime, yet somehow neighboring quarks should be so close that asymptotic freedom applies. The authors of Ref. [35] proposed a solution to this seeming contradiction by postulating that matter in this regime is quarkyonic, with quarklike degrees of freedom deep inside the Fermi surface (and hence a scaling $\sim N_c^1$ for the pressure) but baryonic excitations on the surface.

While the argument above is compelling, it raises somewhat subtle issues about how to characterize matter in the $\sqrt{N_c/N_f}\Lambda_{\mathrm{QCD}} \geqslant \mu_Q \geqslant \Lambda_{\mathrm{QCD}}$ part of the diagram. Above $\mu_Q = \Lambda_{\mathrm{QCD}}$, baryons will conceivably overlap. If quarks are free within baryons, then how does one distinguish the quarkyonic phase from a deconfined phase? Intuition from models such as the bag model [49] does, indeed, suggest that deconfinement happens at $\mu_Q \simeq \Lambda_{\mathrm{QCD}}$, in contrast with Fig. 1 and Ref. [35].

It is clear that *if* color can flow within overlapping baryon regions and asymptotic freedom applies in the large N_c limit, the Wilson loop expectation value within an area covering "many overlapping baryons" will break the area law because, within the overlapping regions, the Gauge field configurations will fluctuate chaotically around a zero average [50,51]. (An

alternative way to see it, originally owing to Ref. [52], is that if Gauge bosons can propagate through overlapping baryons, Gauss' law forces interquark fields to $\sim 1/r^2$.) In this scenario, quarkyonic matter will be essentially deconfined (according to the criteria set in Refs. [50,51] to define confinement), and hence indistinguishable from a QGP, and the picture in Ref. [49] will be correct. This is *possible*, because Fig. 1 does not preclude *nonperturbative* contributions to the running of quark-quark interactions, which could, in principle, bring the critical μ_Q for deconfinement down to $N_c^0 \Lambda_{\mathrm{QCD}}$.

However, as we explore in Sec. IV (and was explored in the past in the context of color superconductivity [53–56]), it is not an inevitable conclusion: Periodic quark wave functions, together with a generalization of spin-charge separation, can provide a physical mechanism whereby quantum numbers associated with quarks can move across arbitrary distances while color itself is confined to a configuration-space scale of ~ 1 fm. In this case, quarkyonic percolation and deconfinement are physically different phases, distinguishable by the usual order parameters associated with confinement.

Of course, it remains to be seen whether such mechanisms are realized in nature, and either possibility (a new phase or a nonperturbative breaking of N_c scaling of the β function) is interesting. In the rest of this work we assume that dynamics of the type in Sec. IV holds, so a regime where color is localized, but quarks of neighboring baryons can interact is possible. We then use the model developed in Ref. [21] to try to define where, in density, temperature, and N_c, this regime can be located, to provide future experimentalists and phenomenologists tools to distinguish between the above possibilities.

The possibility of exploring the quarkyonic transition experimentally further assumes that physics at high chemical potential is qualitatively the same when N_c is varied from 3 to infinity. In Ref. [21] it has been shown that for a wide variety of reasonable propagators at a fixed baryonic number density of $\rho_B = \Lambda_{\mathrm{QCD}}^3/8$ a percolation transition is found as N_c is varied. If one identifies the percolation transition with the quarkyonic phase, deconfinement and percolation are indeed separate, and they cover different regions not just in T and μ_B, but also along N_c.

In this work, we aim to extend the results of Ref. [21] to variable density and nonzero temperature. The purpose of this exercise is to determine the role of percolation in the full T-μ-N_c phase diagram, and to see whether percolation is involved in the physical $N_c = 3$ world, or, instead, whether this transition divides our world from the "truly large-N_c" regime.

Specifically, we aim at determining whether there is a region, in the T-μ_B plane, where a percolating yet confined phase is likely at $N_c = 3$, $\Lambda_{\mathrm{QCD}} \leqslant \mu_Q \leqslant \sqrt{N_c/N_f}\,\Lambda_{\mathrm{QCD}}$. If so,[1] this

---

[1]In our world, of course, $N_f = 2$ if the strange quark is heavy, and $N_f = 3$ if the strange quark is light. Because the bare strange quark mass $\sim \Lambda_{\mathrm{QCD}}$, it is far from clear which limit applies, yet this is the crucial question determining whether N_f/N_c is an expansion parameter *at all*. The mass of the strange quark might well be the crucial *qualitative* uncertain driving factor in our results and hence fundamentally determine the nature of the QCD phase diagram [57, 58].

would be the natural region to investigate for quarkyonic effects in experiment. We also ask ourselves whether percolation is related to the more usual liquid-gas phase transition and if its onset therefore accounts for the large phenomenological failures of the large-N_c picture in this regime [20].

We close with a discussion outlining what an effective theory for percolating matter would look like and suggesting ways of looking for it in both lower energy experiments and astrophysical searches (neutron and proto-neutron stars).

II. THE VARIABLE-DENSITY PERCOLATION MODEL

The strategy used to investigate the percolation properties of high-density baryonic matter is a generalization of the model presented in Ref. [21], to which we refer for further introductory details. In our description, baryonic matter is arranged in a cubic lattice, with a baryon sitting at each lattice site: Its quarks will be randomly, independently positioned according to a hard-sphere distribution with radius $1/\Lambda_{\mathrm{QCD}}$: $f(\mathbf{x}) \propto \Theta(1 - \Lambda_{\mathrm{QCD}}|\mathbf{x} - \mathbf{x}^{\mathrm{center}}|)$. In Ref. [21], each sphere touches exactly its six neighbors, that is, the lattice spacing is fixed to $2/\Lambda_{\mathrm{QCD}}$ and the density $\bar{\rho}$ is therefore fixed (we relate $\bar{\rho}$ to the thermodynamic baryonic density ρ_B in Sec. III). Replacing the cubic arrangement with another regular three-dimensional (3D) lattice would have changed the percolation threshold by $\mathcal{O}(30\%)$ or so [59] and hence not impacted our results qualitatively.

The generalization to a variable-density setting is realized by the introduction of the parameter ϵ, defined as the ratio of the lattice spacing over twice the spheres' radius: Thus, the density $\bar{\rho}_0$ examined in Ref. [21] had $\epsilon = 1$. Because at $\bar{\rho}_0$ each baryon occupies a volume of $(2/\Lambda_{\mathrm{QCD}})^3$, we now have

$$\bar{\rho}(\epsilon) = \bar{\rho}_0 \frac{1}{\epsilon^3} = \frac{\Lambda_{\mathrm{QCD}}^3}{8} \frac{1}{\epsilon^3}. \qquad (1)$$

In support of this classical, static description of baryonic matter, we keep an eye to the large-N_c limit and note that the propagation speed of Fermi-surface baryons, $\sim 1/\sqrt{N_c/N_f}$ in the confined regime, is parametrically smaller than the characteristic momentum of quarks, $\sim N_c^0$; hence, percolating quarks see the baryons as quasistatic (a crystal at larger N_c [2,10], and, presumably, a disordered "glass" at smaller N_c). Deviations from the "baryons are spheres" assumption might become significant when the number of colors approaches the number of neighbors of a densely packed system [20], which in 3D means $N_c \sim \mathcal{O}(10)$. This, as we show, coincides roughly with the percolation threshold for "sensible" choices of the parameters at play.

We note that we are assuming that baryon size does not depend on baryonic density. Seemingly, this assumption is counterintuitive because the pionic corona around the baryon is set by f_π^{-1}, which should decrease as chiral symmetry is partially restored [60]. We note, however, that $f_\pi \sim \sqrt{N_c}$ and hence diverges for all chemical potentials as $N_c \to \infty$. In this limit baryons interact strongly with pions [1,2,61], as strongly, in fact, as with each other (NN interactions via pions scale in the same way as NN interactions via quarks [2]). The

baryon size, however, stays finite and $\simeq \Lambda_{\rm QCD}^{-1}$ in this limit. This suggests that at large N_c the baryon size becomes a lot more dependent on "bag physics"/confinement (and, in general, the scale at which QCD becomes strong) than on the pion corona. Because of this, pion size changes with N_c are, at best, a subleading effect, to be disregarded here. The fact that percolation, as defined here, is primarily an effect of confinement physics, as it survives in a world with only one quark flavor and no mesons, reinforces this conclusion.

Let us briefly summarize the results in Ref. [21] before generalizing to the present setting. We assume a probability ("squared propagator") for two quarks in different baryons to exchange energy/momentum with the essential properties of (a) getting weaker as λ/N_c at increasing N_c and (b) dropping quickly to zero around some confinement scale $r_T/\Lambda_{\rm QCD} \propto \mathcal{O}(1)N_c^0$. These requirements enforce the relevant physics of the problem; we then consider two representative choices for the "propagator," inspired by the Gribov-Zwanziger theory [62,63]: the step function in coordinate space and the step function in momentum space (that is, the squared Fourier transform of a p-space θ function). These can arise out of chromo-field interactions, such as in Refs. [46,47]. Their expression, suitably normalized, is given by

$$F_T(y) = \frac{\lambda}{N_c} \, \Theta\left(1 - \frac{y}{r_T/\Lambda_{\rm QCD}}\right), \qquad (2)$$

$$F_K(y) = \frac{\lambda}{N_c} \frac{2r_T^2}{\pi y^2} \sin^2\left(\frac{y}{r_T/\Lambda_{\rm QCD}}\right)$$

$$\propto \left[\int d{\rm p}\, e^{-ipy}\Theta(p - \Lambda_{\rm QCD}/r_T)\right]^2, \qquad (3)$$

respectively, where y is the interquark distance in physical units. The two parameters are $r_T \sim 1$ and $\lambda \sim 1$ ('t Hooft coupling), controlling, respectively, the range and the intensity of the interquark exchanges.

Conceptually, these definitions leave some ambiguity of what is "propagated." Our working hypothesis is that Eqs. (2) and (3) represent tunneling-driven interactions of quarks from different baryons exchanging conserved quantum numbers (spin, flavor, energy-momentum) concurrently with some global color-neutralization mechanism acting at distance scales $\geqslant \Lambda_{\rm QCD}^{-1}$. We leave discussion as to how this could happen to Sec. IV. We note, however, that similar propagators have already been used in the context of quarkyonic matter, having been instrumental in the study of the conjectured quarkyonic "chiral spirals" [64,65] [the results in Ref. [36] are based on a propagator of the form of Eq. (3)].

With $F(y)$ and $f(\mathbf{x})$ as input, then, a probability p for the exchange between neighboring baryons A and B is computed via

$$p(N_c) = 1 - \left\{\int f_A(\mathbf{x}_A)d^3\mathbf{x}_A \int f_B(\mathbf{x}_B)d^3\mathbf{x}_B \right.$$

$$\left. \times [1 - F(|\mathbf{x}_A - \mathbf{x}_B|)]\right\}^{N_c^\alpha}. \qquad (4)$$

In Ref. [21] we concluded that, to meet the expectation $p \to 1$ for $N_c \to \infty$, the correct choice is $\alpha = 2$: We interpret it as

a cross-baryon "interaction," as opposed to the cross-baryon "propagation" associated with $\alpha = 1$.

Varying baryon density should not alter the $\alpha = 2$ dependence assumed in Ref. [21]: If N_c is large enough, $\alpha = 2$ will obviously always dominate over the $\alpha = 1$ component. Furthermore, as shown in Ref. [21], $\alpha = 1$ would imply a regime where $N_c \to \infty$ matter would be less correlated (and hence less strongly bound) than $N_c \ll \infty$ (the nuclear binding energy dependence of N_c would have a peak at some intermediate N_c and reach the limit of Ref. [2] from above). Because quantum corrections generally make a many-Fermion system more repulsive (by Pauli blocking arguments alone), and because at large N_c attractive channels dominate over repulsive ones, it is difficult to imagine a physical justification for such behavior in either naive N_c counting or gauge/gravity.

At large N_c, therefore, it is natural to expect $\alpha = 2$, but at $N_c = 3$ an $\alpha = 1$ component, negligible at $N_c \to \infty$, could be significant. As the next section makes clear, assuming $\alpha = 2$ throughout can be regarded as an "optimistic limit" for the existence of the percolating phase, and any $\alpha = 1$ admixture will make the percolating phase less likely.

A similar discussion is needed to clarify the role of antibaryons in percolation at $T > 0$. Because by percolation we mean the delocalization of the quark wave function across baryons, as we do in Sec. IV, then only quarks delocalize, because delocalization is brought about not by deconfinement but by the formation of a quark Fermi surface. Antibaryons will then show up as an impurity in the percolation links. We ignore this impurity for the current work, because we are concentrating on the "most optimistic scenario" and any impurity will flatten the ρ_B-N_c percolation curves, making a percolating but deconfined phase less likely. In addition, the probability of having a local impurity $\sim \exp[-N_c] \sim 1\%$ even at the highest temperature $T \simeq T_c$, so its effect should be smaller than other effects we neglect in this work.

The resulting p is a function of N_c (see Ref. [21] for details) and can be compared with the bond-percolation threshold to determine if large-scale correlations occur or not, identifying a critical N_c^* where the system starts to percolate. Note that direct exchange between non-neighboring baryons is neglected by construction.

However, in the variable-density setting, when ϵ is small we have substantial overlapping between the spheres and non-negligible contributions from non-nearest-neighbor direct exchange: We need to take into account a set of baryon-to-baryon probabilities p_i, one for nearest neighbors, one for neighbors with relative distance of $(1, 1, 0)$ spacings, and so on. In practice, we considered nine probabilities $\{p_i, i = 0, \cdots, 8\}$, associated to nine "neighboring classes" (we assume the probability of direct exchange between spheres that are further apart can safely be neglected): The corresponding relative distances, in units of the interbaryonic distance, read

$$(1, 0, 0), (2, 0, 0), (1, 1, 0), (2, 1, 0), (2, 2, 0),$$
$$(1, 1, 1), (2, 1, 1), (2, 2, 1), (2, 2, 2). \qquad (5)$$

Thus, for each choice of the parameters (r_T, λ), each "propagator" and each ϵ, a set of $\{p_i\}$ can be evaluated numerically with Eq. (4) by placing the two centers at the
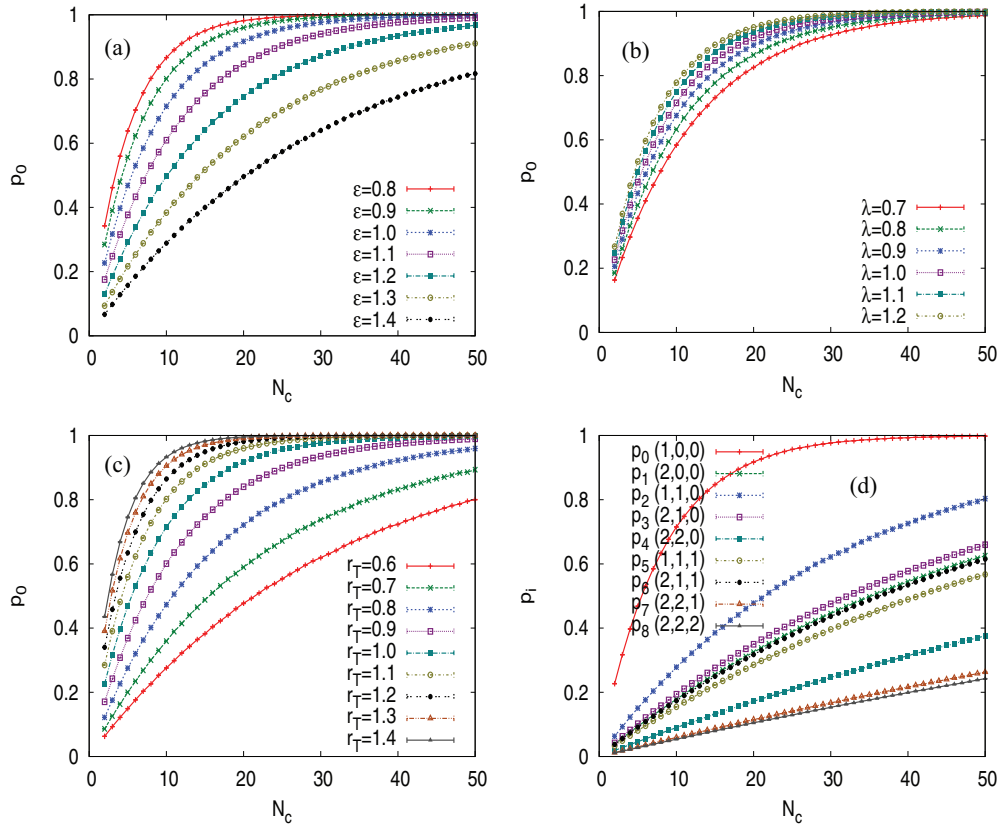
FIG. 3. (Color online) Baryon-to-baryon probabilities for the F_K propagator; the reference case is $\epsilon = r_T = \lambda = 1.00$. (a) p_0 for varying ϵ. (b) p_0 for varying λ. (c) p_0 for varying r_T. (d) p_i at all neighboring classes considered.

desired distance. Representative results are shown in Fig. 3 for the F_K propagator. We examine 9 values of $r_T \in [0.6{:}1.4]$, 6 of $\lambda \in [0.7{:}1.2]$, and 13 of $\epsilon \in [0.8{:}1.4]$: The latter corresponds to ranging in density from $\sim 0.046\Lambda_{\rm QCD}^3$ to $0.244\Lambda_{\rm QCD}^3$. We generate data for all integer N_c from 2 to 80. The $\{p_i\}$ are calculated numerically by sampling the integrand about 4×10^5 times per setup.

The next step is to translate the set $\{p_i\}$ to a single probability p, which will be compared to the 3D cubic-lattice bond-percolation threshold $p_c \simeq 0.2488$. This is accomplished by means of Monte Carlo renormalization (see, e.g., Chapter 4 of Ref. [66]): We perform a blocking step on a cell of b^3 sites, mapping the problem to a superlattice whose sites are the corners of the cell; the corresponding p is evaluated by numerical simulation, with the $\{p_i\}$ as input, as the probability that two opposite planes on the cell are connected by a continuous path. Because p_0 is the only relevant coupling in the blocking-out flow, we are effectively moving on a renormalization group (RG) trajectory in the 9D space of the p_i, whose fixed point—the percolation critical point—lies on the axis $p_i = 0$, $i > 0$. The procedure is illustrated in Fig. 4. In practice, we start with an empty b^3 lattice and, considering all pairs of sites, we switch on the links according to the p_i for the corresponding neighboring class. At the end of the process we can have a continuous path connecting the $z = 0$ wall of the cube with the $z = b - 1$ wall: The probability $p(p_i)$ for this to happen is computed by repeating the operation many times (in our case, 20 000 times per setup).

The exact choice of the "crossing rule" R_1 (that is, we get a 1 if and only if there is a connection between two opposite wall in a chosen direction, ignoring what happens along the other two directions) is arbitrary: for large-enough b, all recipes would lead to the same final result.

In the limit $b \to \infty$, the crossing probability is a step function, zero before percolation and one after percolation. When evaluated exactly at criticality, it assumes a universal value depending only on the crossing rule considered. In 3D, with the R_1 rule, $p^*(b) = \Pi_1 + \beta b^{-y}$ with the limit value $\Pi_1 = 0.265$ [67], and leading correction $b^{1/\nu}$, with $\nu \simeq 0.8765$ the 3D percolation critical exponent.

To check the implied assumption of a b "large enough," cell sides from three to seven lattice steps are employed, and the results compared for stability. This technique is first tested on the 1D subspace of nearest-neighbor-only $p_0 \to p$, where
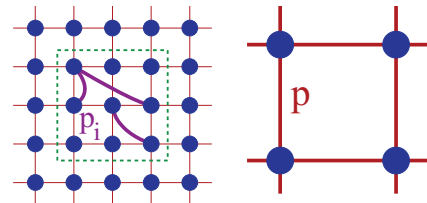

FIG. 4. (Color online) Schematic procedure for the RG step. The $b = 3$ cell on the left, with all its bond probabilities p_i, becomes an elementary square of the superlattice on the right, with the associated p as its only, nearest-neighbor, bond probability.
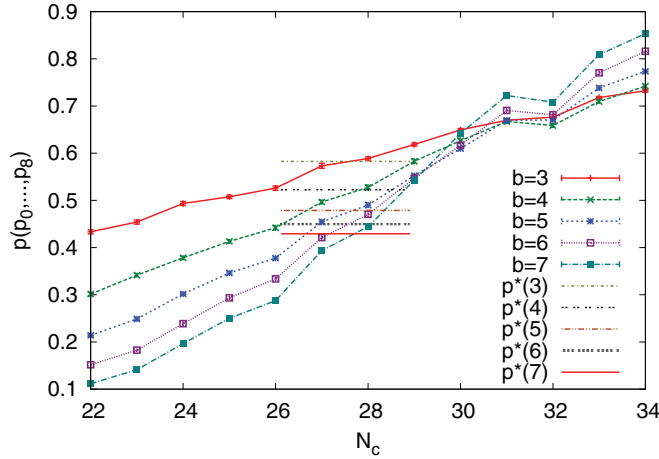
FIG. 5. (Color online) Determination of the b-dependent critical N_c^*, for F_T with $\epsilon = 0.8, \lambda = 0.7, r_T = 0.6$. Horizontal lines mark p^*.

we roughly reproduce the scaling to the large-b limit: Yet, the curves $p_b(p_0)$ have a rather b-dependent value p^* at the critical threshold:

$$p^* = \{0.5825, 0.5226, 0.4788, 0.4488, 0.4293\},$$
$$\text{for} \quad b = 3, 4, 5, 6, 7. \quad (6)$$

This leads us to define an effective, b-dependent critical N_c^*, the value at which the full renormalization step yields the p^* for that cell size (practically found by interpolation). We are satisfied with the procedure whenever N_c^* shows a substantial independence of b; indeed, this will be the case: For example, at $\epsilon = 0.8$, $\lambda = 0.7$ and $r_T = 0.6$, we get for the propagator F_T (cf. Fig. 5)

$$N_c^* = \{27.9, 27.6, 27.9, 27.6, 27.5\}, \quad b = 3, 4, 5, 6, 7. \quad (7)$$

The final result is then obtained by the above population of results. The choice of considering bonds between baryons far apart has, however, a drawback: namely, the propagator F_K [Eq. (3)], as it is, has local maxima around $y\Lambda_{\text{QCD}} \sim \pi r_T, 3\pi r_T$ and so on, which dramatically alters the results in a nonphysical way; the coincidence of the secondary peaks with neighboring positions is, of course, specific to a cubic lattice and should not occur in a disordered "glass of baryons."

More generally, however, the power law "tail" in the propagator makes correlation lengths diverge at $N_c \sim \mathcal{O}(1)$ for densities arbitrarily close to $\mathcal{O}(\Lambda_{\text{QCD}}^3)$. The implementation of such a sharp step propagator in momentum space, however, contradicts our intuition of statistical physics: A probe charge interacting with a statistical medium is generally exponentially screened by charge-hole pairs, acquiring a screening length of dimension $\sim 1/\mu$ (or $\sim 1/T$ for $T \sim \mu$). This is a "universal" feature of interacting systems at equilibrium, because any backreaction of a charge on a field, to first order, will give a similar effect (the absence of such a screening leads to a divergence in the partition function of the fully interacting system; the hydrogenic atom's case is a well-studied example of these classes of phenomena [68,69]). Because $\mu_Q \sim \Lambda_{\text{QCD}}$ in the limit we are using, the propagator should be exponentially screened at a similar scale. Then, in the following, we use a "K" propagator altered by an exponential screening,

$$F_S(y) = \frac{\lambda}{N_c} \frac{2r_T^2}{\pi y^2} \sin^2\left(\frac{y\Lambda_{\text{QCD}}}{r_T}\right) e^{-M|y|}, \quad (8)$$

that is, a F_K times a damping exponential factor whose characteristic length is, in practice, fixed to $1/\Lambda_{\text{QCD}}$. F_S, taking the square root and antitransforming, yields

$$\tilde{g}_S(k) = \int_{-\infty}^{+\infty} dx \sqrt{F_s(x)} e^{ikx} \propto \left\{ \text{atan}\left[\frac{2\Lambda_{\text{QCD}}}{Mr_T}\left(k\frac{r_T}{\Lambda_{\text{QCD}}} + 1\right)\right] - \text{atan}\left[\frac{2\Lambda_{\text{QCD}}}{Mr_T}\left(k\frac{r_T}{\Lambda_{\text{QCD}}} - 1\right)\right]\right\},$$

i.e., a "rounded off" step function in momentum space.

Following the above methodology, we obtain curves in ϵ, one for each propagator (F_T, F_K—later ignored—and F_S) and each (r_T, λ), which can be translated into curves $N_c^*(\bar{\rho})$ through Eq. (1).

Examples of such curves are shown in Fig. 6. We note that they are well fitted to the form

$$N_c^*(\bar{\rho}) = \frac{A}{(\bar{\rho}^Z + B)}. \quad (9)$$

We have shown that the percolation transition line in $\bar{\rho}$-N_c space is strongly curved. This has the potential of dramatically altering the conclusions of Ref. [21], provided the assumption that the relevant density is $\sim \Lambda_{\text{QCD}}^3/8$ is relaxed: At a greater density, provided baryons still exist, N_c^* can very well be lowered from $\mathcal{O}(10)$ to $N_c = 3$, making the percolating phase

accessible to experiment. The existence of baryonic states, of course, implies that the relevant density is still in the confined phase. In Sec. III, therefore, we examine the interplay between the confining and percolating transitions.

III. THE CONFINEMENT PHASE TRANSITION IN N_c-ρ_B-e SPACE

As discussed in the Introduction, if one identifies the density of interest for percolation, $\rho_B \sim \Lambda_{\text{QCD}}^3/8$ (one baryon per baryon size), with the thermodynamic density, then, at $T \ll T_c$, the percolation transition happens firmly in the confined phase in the large-N_c limit because of the μ_Q^2 dependence of the quark-hole screening diagram (Fig. 1).

We also know that, at $T \simeq T_c$—where the chemical potential for deconfinement is zero—, μ_Q does not scale with
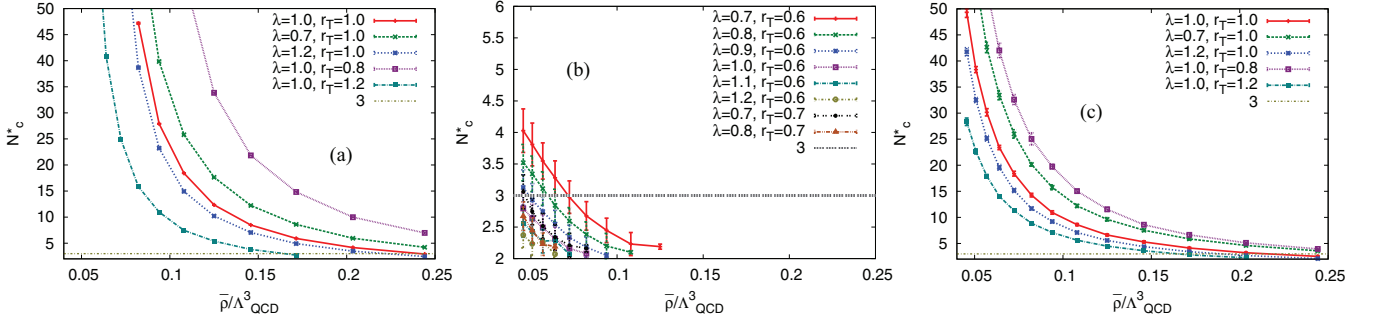
FIG. 6. (Color online) Representative results, with some choices of r_T, λ, for the critical percolation N_c^* as a function of the baryon density, coming from using the propagators F_T of Eq. (2) (a), F_K of Eq. (3) (b), and F_S of Eq. (8) (c).

N_f, N_c. Hence,

$$\mu_Q^{\text{conf}}\big|_{T \ll T_c} = \mathcal{O}(1)\sqrt{\frac{N_c}{N_f}}\Lambda_{\text{QCD}}; \quad \mu_Q^{\text{conf}}\big|_{T \sim T_c} \to 0;$$

$$T_c \simeq \left(\frac{2\Lambda_{\text{QCD}}}{3}\right)N_c^0 N_f^0. \tag{10}$$

In this section, we use the ideal gas ansatz for the nuclear liquid to translate these estimates into an estimate of how ρ_B^{conf} and the energy density e^{conf} depend on N_c. We note that, even in the case of Van der Waals corrections of order $\mathcal{O}(N_c)$, the density ρ_B at a given T will change at most with terms of $\mathcal{O}(1)$ [20] and therefore can be ignored for this calculation.

We start with the ideal gas formula for the density of a relativistic massive gas of fermions,[2]

$$\rho_B = \frac{4\pi g_f g_s}{(2\pi)^3}[B_1(m, T, \mu_B) - B_1(m, T, -\mu_B)], \tag{11}$$

the first term accounting for baryons and the second for antibaryons, with [58,70]

$$B_1(m, T, \mu_B) = \int_0^\infty \frac{p^2 dp}{\exp\left[\frac{1}{T}\left(\sqrt{p^2 + m^2} - \mu_B\right)\right] + 1}$$
$$= \sum_{n=1}^\infty (-1)^n m^2 \frac{T}{n}\exp\left(\frac{n\mu_B}{T}\right)K_2\left(\frac{nm}{T}\right) \tag{12}$$

and $K_n(x) = \int_0^\infty e^{-x\cosh t}\cosh(nt)dt$ the modified Bessel function. The degeneracy terms g_f and g_s are both somewhat nontrivial: g_f counts the total "generalized isospin" states accessible allowed for the baryon, and so is 1 for one flavor and $N_f(N_f - 1)$ for a higher number. If we ignore excited spin states, the baryon will always have spin-$\frac{1}{2}$, so that $g_s(N_c) \equiv 2$; we later refine this simplification.

For $T \ll N_c\Lambda_{\text{QCD}}$ the antibaryon term becomes negligible and the baryon density becomes, in units of "one baryon per

baryon size,"

$$\rho_B = K_0^{3/2}\frac{4}{3}\pi(0.6\text{ fm})^{-3}, \quad \mu_B \simeq 2\pi\left(\frac{3\sqrt{\pi}}{4}\right)^{2/3}\frac{\rho_B^{2/3}}{m},$$
$$\mu_B \simeq 1.7K_0 \text{ GeV}. \tag{13}$$

For $K_0 = 1$ (approximately one baryon per baryon size), this corresponds to the density examined in Ref. [21], where $N_c \sim \mathcal{O}(10)$ is necessary for percolation. We need, therefore, $K_0 > 1$, but not enough to trigger deconfinement.

We note that it is impossible to estimate the $\mathcal{O}(1)$ parameters in Eq. (10), and hence K_0, to better than an order of magnitude: These factors depend on the SU(N_c) structure constants showing up in the two diagrams of the top panel of Fig. 1, as well as the mean-field corrections to the quark and gluon wave functions, which enter in the incoming and outgoing lines in the same top panel of Fig. 1 [71]. The latter are completely undetermined, even for a dilute gas at large N_c [72,73]. Finite temperature and antibaryons will introduce additional modifications of K_0.

Unfortunately, this uncertainty radically limits the predictive power of this section, because, as we shall see, factors of $\mathcal{O}(1)$ are crucial for deciding whether a percolating phase does, in fact, occur at $N_c = 3$. Nevertheless, we shall continue to illustrate the issues at hand.

From Eq. (10), we parametrize the zero-temperature baryonic chemical potential needed for deconfinement as

$$\mu_0 = \mu_B^{\text{conf}}(T \ll m) = \mathcal{O}(1)N_c^{3/2}N_f^{-1/2}\Lambda_{\text{QCD}} \tag{14}$$

(roughly $N_c^{1/2}N_f^{-1/2}$ baryons need to overlap), and the baryon mass is $m \sim N_c\Lambda_{\text{QCD}}$. Omitting such factors of $\mathcal{O}(1)$, we are led to change the variables to

$$\gamma = \frac{\sqrt{N_c}}{\mu_0}m, \quad \alpha = \frac{\sqrt{N_c}}{\mu_0}p, \quad \beta = \frac{\Lambda_{\text{QCD}}}{T}\frac{N_c}{\sqrt{N_f}}; \tag{15}$$

note that at zero-temperature deconfinement we have $\beta \to \infty$ and $\gamma = \sqrt{N_f}$. We write the critical ρ_B^{conf} for confinement as

$$\rho_B^{\text{conf}}\left(\beta \gg \Lambda_{\text{QCD}}^{-1}\right) = \frac{4\pi g_f g_s}{(2\pi)^3}\frac{N_c^3}{N_f^{3/2}}\Lambda_{\text{QCD}}^3 B_2(N_c, \gamma, \beta), \tag{16}$$

---

[2]For "baryons" to be fermions, we should limit ourselves to integer, odd N_c, as long as we do not include the excited spin states; however, the formulas are valid—and have here been calculated—for generic positive values of N_c.

where

$$B_2(N_c, \gamma, \beta) = \int \frac{\alpha^2 d\alpha}{1 + \exp\left[\beta\left(\sqrt{\alpha^2 + \gamma^2} - \sqrt{N_c}\frac{\mu}{\mu_0}\right)\right]} - \int \{\text{same with } \mu \to -\mu\}$$

$$= \sum_{n=1}^{\infty} (-1)^n \frac{n\gamma^2}{\beta} \sinh\left[\left(\sqrt{N_c}\frac{\mu}{\mu_0}\beta\right)^n\right] K_2(n\gamma\beta). \tag{17}$$

This is the general expression for the baryon density at deconfinement as a function of N_c. For very low temperatures ($\beta \to \infty$, $\mu = \mu_0$), the second term in B_2 vanishes and the exponential at the bottom of the first term is infinity if $\chi > 0$ and zero if $\chi < 0$, where

$$\chi = \sqrt{\gamma^2 + \alpha^2} - \sqrt{N_c} = \sqrt{\alpha^2 + N_f} - \sqrt{N_c}. \tag{18}$$

We then get easily the low-temperature behavior:

$$\rho_B^{\text{conf}}(T = 0) = \Lambda_{\text{QCD}}^3 \frac{1}{6\pi^2} g_f g_s \frac{N_c^3}{N_f^{3/2}} (N_c - N_f)^{3/2}$$

$$\sim \frac{g_f g_s}{6\pi^2} \Lambda_{\text{QCD}}^3 \frac{N_c^{9/2}}{N_f^{3/2}}. \tag{19}$$

At $T = 0$, ground-state baryons are the *only* possible hadronic degrees of freedom of the system. Hence, one can trivially identify ρ_B with the $\overline{\rho}$ of Sec. II and directly compare deconfinement with percolation: This is done in Fig. 7. In contrast to what we find in Ref. [21], it seems that a confined but percolating density at $N_c = 3$ is possible. The discussion in Sec. II elucidates what Ref. [21] missed: Because of the curvature of the density in ρ_B-N_c space, the critical N_c drops very rapidly with density, while the density required for deconfinement rises with N_c. However, the conclusion made in Refs. [20,21] still stands in that the densities required for it are well away from normal nuclear density, as in the large-N_c limit. Hence, percolation is well distinct from the nuclear liquid-gas

phase transition and might not arise if the strange quark is "too light" (see footnote 1). To extend our knowledge to nonzero temperature, we choose the simplest parametrization for the deconfinement line in the T-μ_B plane, i.e., that of a quarter of an ellipse whose radii are given by the known points $T = T_c$ and $T = 0$:

$$1 - \theta^2 = \left(\frac{\mu_B^{\text{conf}}}{\mu_0}\right)^2, \quad \theta = \frac{T}{T_c} \simeq \frac{3}{2}\frac{T}{\Lambda_{\text{QCD}}}. \tag{20}$$

Considering that the transition line is given by the interplay of the matrix elements shown in Fig. 1, this elliptical parametrization is actually physically well motivated, although it misses the $\sim T\mu$ interference between screening and antiscreening.

When raising the temperature, we should also include states of higher spin in our calculation: In the large-N_c limit, a spin flip has a cost of $\sim \Lambda_{\text{QCD}}/N_c$ [74], and there can be up to $(N_c - 1)/2$ of them.[3] We now assume $N_c = 2Q + 1$ odd integer and introduce a sum over spin states parametrized by $\eta = 0, 1, \ldots, Q$ (in this way, neglecting higher-spin states amounts to limiting all sums to $\eta = 0$), each carrying its degeneracy $(2\eta + 2)$: This setup replaces the factor g_s of Eq. (11). Thus, we write, for nonzero temperature and including higher spins, the density as

---

[3]Admittedly, here we prefer to keep the model simple despite the fact that in our $N_c = 3$ world the cost of flipping, say, a proton into a Δ^+ is around Λ_{QCD} and not $\Lambda_{\text{QCD}}/3$.

$$\rho_B^{\text{conf}} = \frac{4\pi g_f}{(2\pi)^3} \frac{N_c^3}{N_f^{3/2}} \Lambda_{\text{QCD}}^3 \sum_{\eta=0,1\ldots}^{Q} (2\eta + 2) \left\{ \int \frac{\alpha^2 d\alpha}{1 + \exp\left[\frac{3}{2}\frac{N_c}{\sqrt{N_f}}\frac{1}{\theta}\left(\sqrt{\alpha^2 + N_f} + \eta\frac{\sqrt{N_f}}{N_c^2} - \sqrt{N_c}\sqrt{1 - \theta^2}\right)\right]} \right.$$

$$\left. - \int \frac{\alpha^2 d\alpha}{1 + \exp\left[\frac{3}{2}\frac{N_c}{\sqrt{N_f}}\frac{1}{\theta}\left(\sqrt{\alpha^2 + N_f} + \eta\frac{\sqrt{N_f}}{N_c^2} + \sqrt{N_c}\sqrt{1 - \theta^2}\right)\right]} \right\}. \tag{21}$$

This relation is plotted in Fig. 8, top panels. As temperature and N_c rise, less and less energy density is carried by baryons, because the hadronic degrees of freedom are light mesons (of mass $\leqslant 2\Lambda_{\text{QCD}}$) carrying no baryonic quantum number and heavy baryons ($\sim N_c\Lambda_{\text{QCD}}$). The critical energy density e^{conf}, neglecting the meson mass, is

$$e^{\text{conf}} = N_f^2 \frac{\pi^2}{15} T^4 + e_B^{\text{conf}}, \tag{22}$$

with the baryonic contribution given by

$$e_B^{\text{conf}} = \frac{4\pi g_f}{(2\pi)^3} \frac{N_c^4}{N_f^2} \Lambda_{\text{QCD}}^4 \sum_\eta (2\eta + 2) \left\{ \int \frac{\alpha^2 \left[\sqrt{\alpha^2 + N_f} + \eta \frac{\sqrt{N_f}}{N_c^2}\right] d\alpha}{1 + \exp\left[\frac{3}{2} \frac{N_c}{\sqrt{N_f}} \frac{1}{\theta}\left(\sqrt{\alpha^2 + N_f} + \eta \frac{\sqrt{N_f}}{N_c^2} - \sqrt{N_c}\sqrt{1 - \theta^2}\right)\right]} \right.$$
$$\left. + \int \frac{\alpha^2 \left[\sqrt{\alpha^2 + N_f} + \eta \frac{\sqrt{N_f}}{N_c^2}\right] d\alpha}{1 + \exp\left[\frac{3}{2} \frac{N_c}{\sqrt{N_f}} \frac{1}{\theta}\left(\sqrt{\alpha^2 + N_f} + \eta \frac{\sqrt{N_f}}{N_c^2} + \sqrt{N_c}\sqrt{1 - \theta^2}\right)\right]} \right\}. \tag{23}$$

In the e-N_c plane, at T_c, the deconfinement line,

$$e^{\text{conf}}(T_c) = N_f^2 \frac{\pi^2}{15} T_c^4 \tag{24}$$

(with $T_c = 165$ MeV or so [8,9]), is independent of N_c (a vertical line), with a mixed phase in the region

$$N_f^2 \frac{\pi^2}{15} T_c^4 < e < \left(N_c^2 + \frac{7}{8} N_c N_f\right) \frac{\pi^2}{15} T_c^2. \tag{25}$$

At $T \to 0$ (that is, $\theta \to 0$), the line is found by solving Eq. (23) and, similar to the plane shown in Fig. 7, with all energy carried by baryons, in this case we have $e = e_B$. For intermediate temperatures, solving Eq. (23) into Eq. (22) will give an intermediate solution, with a nontrivial approach to the $T = T_c$ case for different N_c; see Fig. 8, bottom panels. The behavior of the energy density is the reason why all curves "curve" (anticorrelate) for low to moderate N_c values in N_c-ρ_B space: At moderate N_c (including our $N_c = 3$ world) baryons

carry a non-negligible fraction of the energy density even in the vacuum phase, with the flavor and spin degeneracy factors beating thermal suppression. At high N_c, while of course baryons continue to carry the baryonic number, mesons carry the bulk of the energy density. Because the scaling with N_c of the deconfinement line is very sensitive to where one is in e-ρ_B [as per Eq. (20)], this interplay can, at lower N_c, change the N_c-ρ_B correlation of confinement into an anticorrelation.

At $T > 0$ baryonic density and energy density are not the parameters driving the percolation phase transition anymore. The way percolation treats baryons in Sec. II does not distinguish between baryons created through chemical potential, whose number is conserved on average, and baryons created in pairs, whose number fluctuates. Each baryon can give rise to quark tunneling and therefore participate in percolating links.

Therefore, and consistently with the discussion in Sec. II, recast the deconfinement curve in the $\overline{\rho}$-N_c plane, where from Eq. (21) we define

$$\overline{\rho} = \frac{g_f}{2\pi^2} \frac{N_c^3}{N_f^{3/2}} \Lambda_{\text{QCD}}^3 \sum_\eta \int \frac{(2\eta + 2)\alpha^2 d\alpha}{1 + \exp\left[\frac{3}{2} \frac{N_c}{\sqrt{N_f}} \frac{1}{\theta}\left(\sqrt{\alpha^2 + N_f} + \eta \frac{\sqrt{N_f}}{N_c^2} - \sqrt{N_c}\sqrt{1 - \theta^2}\right)\right]}. \tag{26}$$

At $T = 0$, where the antibaryon density is strictly zero, these distinctions are insignificant, and the comparison in Fig. 7 suffers no problem. At $T > 0$, however, in principle, we need to use the temperature and chemical potential to calculate the relevant nonconserved quantity. The final result is shown in Fig. 9. As can be seen, the deconfinement line on the new axis is quantitatively very similar to the upper two panels in Fig. 8. Then, the two cases in the previous paragraph yield virtually identical regimes on the phase diagram.

From Figs. 7 and 9 we see that, in the T-μ_B-N_c space, there can be three distinct phases: confined, deconfined, and confined but percolating. In the latter case, arising at high N_c, the Polyakov loop expectation value is still zero and baryons are still physical degrees of freedom but $\langle q(x)\overline{q}(x')\rangle$

should not vanish at scales larger than the baryon size owing to tunneling-driven quark interactions across asymptotically large distances. At low N_c, the confinement density is lower than the percolation density. Because the percolation transition necessitates baryons as physical states, it therefore does not occur, and quarkyonic phases such as in Ref. [35] are not realized.

The critical N_c allowing for a distinction between deconfinement and percolation is typically $\mathcal{O}(10^0)$ at $\theta \ll 1$ and $\mathcal{O}(10^1)$ at $\theta \simeq 1$. Hence, the percolation phase at $N_c = 3$ is accessible at $T \ll \Lambda_{\text{QCD}}$, but at nuclear densities about 2–3 times that of the liquid phase, which, at least using the scaling of Eq. (10), are not yet confining. This regime is somewhat lower in T than that examined in, e.g., Refs. [37,39,40], making
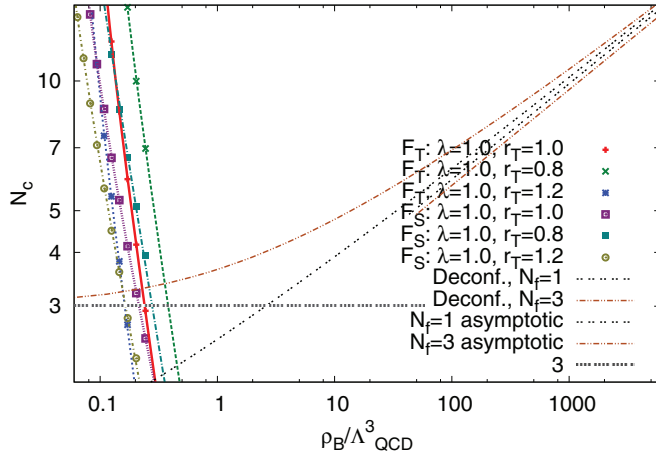
FIG. 7. (Color online) Log-log plot of zero-temperature deconfinement curves versus percolation curves in the plane of $\rho_B \simeq \bar{\rho}$ and N_c. The deconfinement curves [Eq. (19)] are calculated for $N_f = 1, 3$ and are compared to their large-N_c asymptotic form. The percolation curves are shown with their parametrization from Eq. (9).

it likely that percolation dynamics is relevant in proto-neutron stars (a similar regime to that examined in Refs. [75,76]) rather

than lower energy colliders [42–45]. In fact, given that at $N_f = N_c$ deconfinement and nuclear matter parametrically coincide, the crucial parameter determining the existence of a confined but percolating phase, rather than an "early deconfinement" at $\mu_Q \sim \Lambda_{\text{QCD}}$, might be the strange quark mass [57,58]. A further uncertainty is the influence of the $\alpha = 1$ component [see Eq. (4) and following discussion]. If at $N_c \sim 3$ this component dominates, the percolation N_c-ρ_B line is considerably less flat than shown in Fig. 9 (note the different orientation of the N_c axis in Figs. 3 and 9), while the deconfinement line is unaffected. This has the effect of increasing the "critical N_c," where deconfinement and percolation cross; hence, just as in the case of a "light strange quark" or in the presence of antibaryons, a physical percolating but confined phase becomes less likely.

Given the quantitative roughness of the models considered here, however, these are in no way definite conclusions. If anything, these results are much more encouraging for phenomenology than those of Ref. [21], which suggested that at $N_c = 3$ the percolating regime was strictly inaccessible. Given the uncertainties illustrated above, we devote the next two Secs. IV and V, to exploring some theoretical and phenomenological aspects of the percolating phase, in view of giving both experimentalists and astrophysicists some
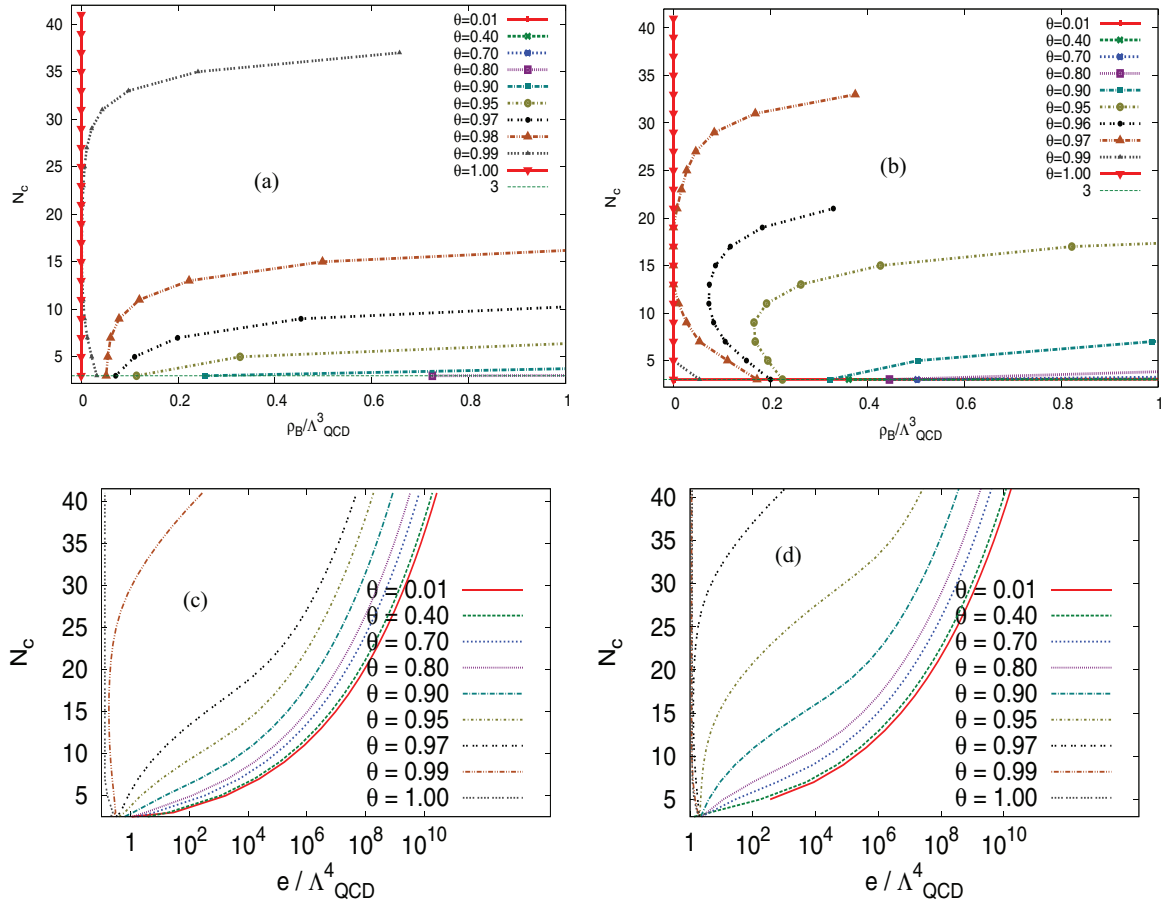

FIG. 8. (Color online) (a),(b) Deconfinement line in the ρ_B-N_c plane according to Eq. (21). (c),(d) Deconfinement line in the e-N_c plane from Eqs. (22) and (23). The plots are for $N_f = 1$ (a),(c) and $N_f = 3$ (b),(d) and for various temperatures spanning $0 < T \leqslant T_c$ (denoted by their θ).
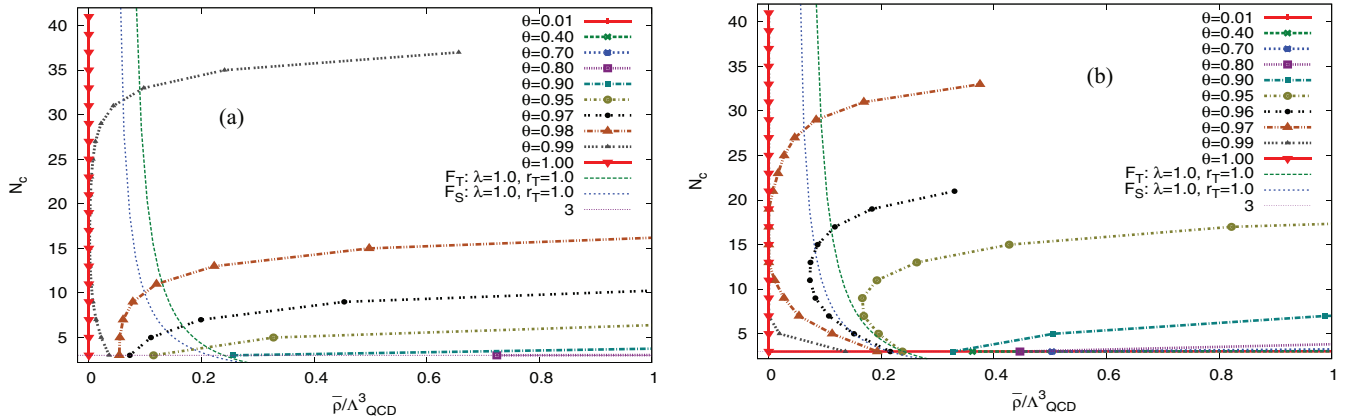
FIG. 9. (Color online) Percolation and deconfinement as a function of $\overline{\rho}$ [defined in Eq. (26)] for one flavor (a) and three flavors (b).

insight into how this phase could manifest and sketching what the effective theory of this percolating phase might be like.

We close this section by comparing the percolating phase to the more "usual" nuclear matter in the large-N_c limit. One can ask how the phase considered here overlaps with the transition between the classical baryonic crystal considered in Ref. [10] and normal nuclear matter. The equivalence between the percolation transition and the onset of the classical regime for baryon dynamics cannot be exact, because percolation is insensitive to the number of flavors (as long as $N_f \geqslant 1$, required for baryons to exist), while the transition is driven not by $N_c/N_N \gg 1$ but rather $N_c/(N_f N_N) \gg 1$, where N_N is the number of neighbors in a closely packed system [20].

However, the interplay between this transition and deconfinement has a similar, albeit weaker, dependence on N_f ($\sim N_f^{-1/2}$ rather than $\sim N_f^{-1}$). Because the critical N_c for this transition is of $\mathcal{O}(10)$, the two transitions do approximately coincide for $N_f \sim \mathcal{O}(1)$. This suggests that varying N_c and N_f separately could yield extremely nontrivial dynamics. Such an "experiment," of course, is possible only on the lattice, perhaps by applying the strong-coupling methods of Ref. [19] to the large-N_c limit [23,24].

IV. EFFECTIVE THEORY OF THE PERCOLATING PHASE

In this work we have used a simple but universal model, motivated by what we know about N_c scaling of the thermodynamics of Yang-Mills theories, to map the interplay of percolation and deconfinement across density, temperature, and number of colors N_c. We found a hitherto-unexplored percolating phase, where confinement persists (the Polyakov loop expectation value vanishes and baryons exist as semi-classical soliton states) but quarks are able to propagate to arbitrarily high distances via interbaryon tunneling, whose probability is governed by a nonperturbative color-neutralizing propagator à la [7,62,63]. Because of this, perturbative quarks

and holes should be able to coexist at momenta $\sim \Lambda_{QCD}$ in the background of baryonic "classical" potential wells.

While, in many ways, our phase bears similarities to the quarkyonic phase conjectured in Ref. [35] and explored in Refs. [36,64,65], there are also differences: In the quarkyonic phase, excitations about the Fermi surface are assumed to be $\sim N_c^0$ at *all momenta*, and hence entropy continues to be $\sim N_c^0$, because sub-Fermi surface states carry no entropy. However, the Gibbs-Duhem relation, linking energy density e and conserved charge density ρ_B to pressure P and entropy density s,

$$s = \frac{dP}{dT} = \frac{P + e - \mu_B \rho_B}{T}, \qquad (27)$$

seems to demand a $s \sim N_c$ scaling in an interacting phase where $P \sim N_c$. If the pressure scales as $P \sim N_c f(T)$, then the only way to avoid entropy density to scale as $\sim N_c$ is to have an equation of state strictly of the form

$$P = N_c^0 f_1(\mu_B, T) + N_c^1 f_2(\mu_B) \qquad (28)$$

(*without* temperature dependence of sub-Fermi degrees of freedom). At $T = 0$ this is certainly the case, but quark-hole diagrams such as in Fig. 10 will inevitably add $\sim N_c f(\mu_B T)$ terms to the partition function, representing excited quark-hole states. Exciting these states will cost momentum $\sim \rho_B^{-1/3}/N_c \sim N_c^\alpha \Lambda_{QCD}$ with $\alpha < 1/2$; hence, it is is not suppressed in the percolating phase. Therefore, perturbations around the Fermi surface could still be colored, but confinement should be maintained at superbaryonic distances. Provided we come up with a physical way to realize such a system, it is a reasonable way of identifying the percolation transition demonstrated here with the phase conjectured in Ref. [35].

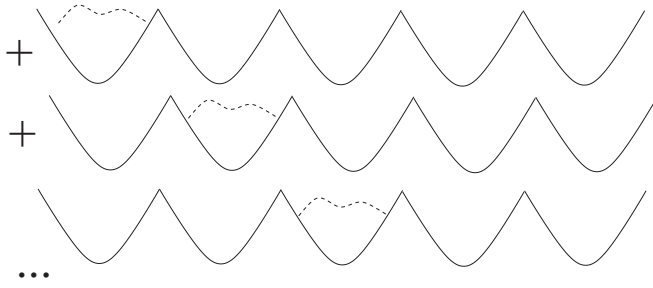FIG. 10. A typical diagram introducing a temperature dependence on the pressure.

FIG. 11. An illustration of the "free quark" wave functions of the percolating phase. Baryons play the role of semiclassical potentials and analogously to atoms in a conductor. Quark wave functions are delocalized by tunneling, and their Eigenstates are in superposition, analogously to electrons. Below percolation, tunneling probability diverges for an infinitely large system, so quarks remain localized with an $\mathcal{O}(1)$ baryonic cluster.

A physical analogy arising from condensed-matter physics is the metal-insulator transition:[4] The critical point of this transition can be understood as percolation of electrons across the semiclassical potential wells generated by the atoms of the material [77]. Tunneling probabilities, as well as electron-electron interactions, are what drive this transition. The analogy with the picture presented here, with the baryons taking place of the atoms, is immediate. In this picture, the low-N_c confined system can only be an "insulator," with quarks of different hadrons not interacting or propagating. At high N_c, however, a "confined conductor" phase is possible, in which the low-energy degrees of freedom are not N_c^0 heavy baryons, but $\sim N_c$ quark-hole pairs: The quarks and holes are confined in hadrons but, owing to tunneling, cannot be univocally assigned to a given hadron. The free energy eigenstates are therefore *superpositions* of quasiparticle quark wave functions across the whole system, with characteristic momentum $k \sim \Lambda_{\text{QCD}}$, in the same way as the free energy eigenstates of electrons in a metal are delocalized: The "free particle" quark, hole (q,h) wave functions (combining color, flavor, and spin) are not a continuum in k but obey the Bloch constraint

$$\Psi_{q,h}^k \big(x + \rho_B^{-1/3}\big) = \Psi_{q,h}^k(x) \exp\big[ik\rho_B^{-1/3}\big]; \qquad (29)$$

this forces the spectral function $\rho_q(k)$ to be of the form

$$\rho_q(k) \simeq \sum_{n=0}^{\infty} \rho_q^n\big(nk\rho_B^{-1/3}\big), \qquad (30)$$

where $\rho_q^n(k)$ is a Lorentzian-type function. Diagrammatically, this is shown in Fig. 11, where the solid lines represent the semiclassical "mean-field" baryon potentials and the dashed lines represent the delocalized quark wave functions. Even if N_c is "high enough" for pQCD quark-hole dynamics to be

relevant, this density of states is radically different from that of a free thermal quark-gluon plasma at high chemical potential, where the spectral function is approximately constant, $\rho_q(k) \sim k^0$.

The combination between the asymptotically free nearly massless quarks with a spectral function inhomogeneous in momentum space such as Eq. (30) is what ultimately enables the chiral inhomogeneities found in Refs. [64,65] and also in models such as Refs. [78,79] and Refs. [46,47]. If such "conductive" quarks are in the asymptotic freedom regime in some limit, their dynamics can be computed perturbatively by adding form factors to quark propagators. For scattering processes (such as quark-hole scattering of Fig. 13 and the virtual excited quark of Fig. 10) the quark and hole propagators will acquire form factors $\widetilde{F}(k)$ (Fig. 12),

$$\frac{k_0^{n-2}}{k^n} \to \frac{(\widetilde{F}(k))^2 k_0^{n-2}}{k^n}. \qquad (31)$$

$n = 2$ would describe a 3D quasiperturbative regime, while $n = 4$ would be close to the Gribov limit described in Sec. II. The propagators of the non-Abelian degrees of freedom in Eq. (33) would be similarly modified. The form factor $\widetilde{F}(k)$ would be the Fourier transform of the lattice of nucleon mean fields shown in Fig. 11. If quark wave functions are of the form of Eq. (29), then lower Fourier components $\Psi_{q,h}^k(x)$ can be color singlets (note that the lowest mode is $\sim \rho_B^{1/3}$), while the higher modes are allowed to be colored, provided a compensating mechanism (such as in Refs. [54–56]) exists, neutralizing the color perturbations over scales larger than $\Lambda_{\text{QCD}}^{-1}$. Such color compensation must actually exist in the QGP as well to avoid paradoxes described, for example, in Ref. [80]; however, such sub-Λ_{QCD} correlations in the high-temperature regime would be negligible for any thermodynamic property of the deconfined phase, because the microscopic scale of this system is above confinement $\sim 1/(N_c^2 N_f T) \ll \Lambda_{\text{QCD}}^{-1}$. This is not so obvious in a confined but quarkyonic phase; we therefore must invent a way for $P, s \sim N_c$ to hold at $T \leqslant T_c$ and yet color neutrality be maintained at scales $\leqslant \Lambda_{\text{QCD}}$.

Condensed-matter physics gives us another example of how this could work, namely, spin-charge separation in 1D systems [81,82] (an effect that does indeed seem to be found in non-Abelian gauge theories [83,84]): In a 1D interacting fermion chain, spin and charge generally separate. If, as suggested in Refs. [64,65], quarkyonic matter is governed by dimensional reduction, such separation could provide the neutralizing force: Confinement would localize the color part of the wave function only, while allowing spin and charge to propagate as N_c copies of a color-singlet field.
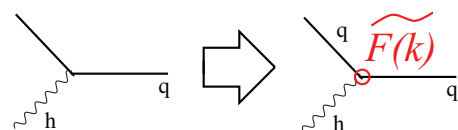
---

[4]Note that this analogy is not perfect, at least because the critical exponents of metal-insulator and percolation are different; in percolation only the two-point correlation is relevant, while typically in metal-insulator transitions higher order correlation functions play a part. The source terms in Eq. (33) could be used to represent such terms.

FIG. 12. (Color online) The difference between free-theory and quarkyonic-theory Feynman diagram expansions. The form factor $\widetilde{F}(k)$ is approximately the Fourier transform of the potential in Fig. 11.
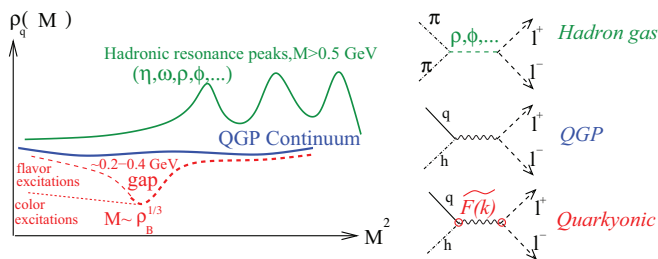
FIG. 13. (Color online) Sketch of what the $\ell^+\ell^-$ spectral function could look like in percolating quarkyonic matter, in a QGP and in a resonance-dominated hadron gas. The gap in quarkyonic matter arises because no delocalized free quark states can exist around $k \sim \rho_B^{1/3}$ [the form factor in Eq. (31) vanishes]. At frequencies below the gap the color part of the wave function stops contributing, but the flavor part might still be present.

While the quantitative development of such a theory is left for future work, we present a sketch of how this works. We use the approach of Ref. [64]; the effective Lagrangian along an infinite percolating chain of quarks will reduce, for N_c colors and N_f flavors, to

$$S = S_{2N_f}[h_{\text{color}}] + S_{N_c}[h_{\text{flavor}}], \qquad (32)$$

where $h_{\text{flavor,color}}$ are separate "flavor" and "color" fields; note that each comes with "redundant" copies of the other.

Neglecting color neutralization, both S_{2Nf} and S_{Nc} should have the following WZNW-inspired form [36,64,85–93]:

$$S_k[\ell] = k \, \text{tr} \left[\frac{1}{16\pi} \int d^2x \; f(x, \ell, \partial_\mu \ell) \partial_\mu \ell \partial^\mu \ell^{-1} \right.$$
$$\left. + \frac{1}{24\pi} \int d^3x \; \epsilon^{\mu\nu\lambda} (\ell^{-1}\partial_\mu \ell)(\ell^{-1}\partial_\nu \ell)(\ell^{-1}\partial_\lambda \ell) \right]$$
$$+ J_{\text{branch}}. \qquad (33)$$

The charges coming in and out of each effectively 1D chain through the branching of the percolation clusters can be represented by source terms J_{branch}. At the percolation transition, they can be defined by the requirement of the 3D conformal invariance of the system.

If $f(x, \ell, \partial_\mu \ell) = 1$, reduces to the Lagrangian of [85–93], and this will be approximately the case for the flavor part. For the color part, however, $f(\cdots) = g(x)h(\ell, \partial_\mu \ell)$ can be used as a mean field.

Baryons can be represented by "mean-field wells," having the form

$$\langle g \rangle(x) = G_0 \left(1 - \sum \hat{g}_n(x) e^{in\rho_B^{1/3}} \right), \qquad (34)$$

where $G_0 \sim N_c$. This forces any wave function for ℓ to be centered around Eq. (29).

Neutralization can be enforced by making $f(x, \ell, \partial_\mu \ell) = 1$ trigger a large background field [54] for color nonsinglet states of momentum $p > \Lambda_{\text{QCD}}$. This effective mass could behave in a similar way as the color chemical potentials discussed in Refs. [55,56].

It can be seen that, with this ansatz, N_c "flavor" excitations of arbitrary frequency and "color" excitations of momentum $k \sim \Lambda_{\text{QCD}}$ survive. For large N_c, these will dominate the entropy.

We thus recovered the premises of Ref. [35], with equations such as (2) as a phenomenological form of the mean-field compensator $f(x, p)$. We therefore arrive, *from the percolating side*, at a consistent physical justification of the ansätze used in the first part of the paper. When N_c is below the percolation threshold, Eq. (29) becomes unphysical, because the probability of the wave function to tunnel more than one baryonic distance is vanishing. Above the percolation threshold, quark wave functions are assigned not to a baryon, but to *all* baryons in an infinite percolating chain following Eq. (29). Quark-hole excitations will obey an effective action given by Eq. (32). In thermal equilibrium, the flavor part of the wave function should yield entropy and pressure $\sim N_c$ even if color is neutral at superbaryonic scales.

Why has nothing similar been observed in gauge/string duality, and how *can* this phenomenon be characterized in such a picture? Because the percolation transition itself is driven by N_c, to model the percolation point one would have to include leading-order g_s corrections, where g_s is the string coupling constant [21]. The percolating phase, however, is in the *low-g_s* limit and therefore could, in principle, be seen by constructions which include baryons in the semiclassical gravity limit, such as Refs. [26,94]. Yet nothing in these works suggests that the dense phase is anything different from a "dense nuclear gas." Quark wave functions might be delocalized, yet this results in no additional degrees of freedom at the level of the entropy density and pressure.

The problem is that the argument in Ref. [35] assumes asymptotic freedom. Even implementations such as Klebanov-Strassler [95,96] do not have asymptotic freedom but rather asymptotic $\mathcal{N} = 4$ SYM with large λ for "hard" momentum exchange. If this transition will appear in gauge/string duality, it will be subleading in α'. The percolating regime occurs at low g_s (high N_c) but higher string tension α' (lower λ), while the "nuclear-matter" phase discussed in Refs. [25,26] happens in the weak limit of both g_s and α'.

Typically, in gauge/string constructions [25,26,94] baryons are represented by stacks of $D7$-branes, with the nuclear-matter phase being represented as a deformation of a string hanging from charged D-branes owing to the charge on the brane [25]. The extra entropy scaling of quarkyonic matter must therefore be driven, in the gauge/gravity picture, by the appearance of Kaluza-Klein modes in such a hanging string. We conjecture, therefore, that quarkyonic matter of the type we discuss arises at low g_s and moderate α'. Subleading corrections in g_s will give rise to the N_c percolation transition between percolating and nonpercolating matter [21] and perhaps the baryon quantum-to-classical transition discussed in Ref. [20].

V. PHENOMENOLOGY OF THE PERCOLATING PHASE

Our calculations show that seeing this phase transition in future experiments in our $N_c = 3$ world [42–45] *might* be

possible, provided low-T, high-ρ_B regions are accessible. This makes it desirable to extend the above discussion and develop some phenomenology for the percolating phase. As in Sec. IV, the quantitative aspect of this is left for future work [71], but we can let the analogy with the metal-insulator transition guide us: A universal characteristic signature of such a system is the appearance of band gaps in the spectral function of charge carriers owing to Eq. (30) and the (weak) interactions between neighboring charge carriers [97]. This discussion is based on the assumption that baryon distributions in quarkyonic matter are more or less regular, allowing for regular band gaps in momentum space to form. While this might not be unreasonable at high density [98], as shown in Ref. [71], irregularities can introduce chaotic event-by-event fluctuations in electromagnetic form factors. A more quantitative calculation is needed to assess the effect of these.

Such band gaps, of mass $\sim$250–400 MeV (well below any resonance mass) could be directly detected in electromagnetic probes (the spectral function of e^+e^- pairs in heavy-ion collisions): As the sketch in Fig. 13 shows, common q hole $\to \gamma \to l^+l^-$ scattering will give an approximately flat spectral function for an unperturbed high-μ QGP. If quark wave functions are delocalized across potential wells of size $\sim \Lambda_{QCD}$, $M^2 \sim \rho_B^{2/3}$ will be suppressed, analogously to the scattering of x rays by electrons in a conducting metal, owing to the suppression of delocalized quark states around that frequency: The form factors of Eq. (31) will be $\widetilde{F}(k = 1/\rho_B^{-1/3}) \ll 1$, and that will depress the scattering cross section shown in Fig. 13. Below that frequency, color-neutralizing effects might suppress the color part of the spectral function, but the flavor part of the spectral function can still contribute.

Heavy-ion collisions at CERN Super Proton Synchrotron and BNL Relativistic Heavy Ion Collider energies have yielded a continuum reminiscent of the QGP spectral function [99,100] on the top of peaks associated to the decay of hadronic resonances (ω, ρ, η, . . .), so perhaps the band gap structure can be sought in upcoming lower energy experiments [42–45].

Alternatively, quarkyonic percolation as described here could be detected in the phenomenology of neutron stars and proto-neutron stars [75,76]. Quarkyonic matter would appear at a pressure about $\sim N_c = 3$ times that of nuclear matter at the same density, temperature, and chemical potential, while maintaining a heat capacity and an energy density comparable to that of nuclear matter. The extra boost in pressure is analogous to the way the electron gas dominates pressure in a metal. Such stiffer equations of state are desirable for stars such as those reported in [101].[5]

Furthermore, a quarkyonic phase in *proto*-neutron stars might be crucial in the dynamics of supernovae. The effective stiffening of the equation of state might affect the early postbounce supernova dynamics and/or black hole formation times during the core-collapse of massive stars. The first effect is interesting in connection to the shock-stalling problem found in, e.g., Ref. [102]. In Refs. [75,76] this problem was solved with a more traditional deconfinement transition, making the equation of state *softer*, because both equilibrium energy density and pressure increase at deconfinement, and the mixed phase drives the speed of sound to zero.

The percolation transition looks significantly different in a way that might make it easier to maintain a shock wave. In the $N_c \to \infty$ limit the phase transition line is vertical in the T-μ_B plane (regions I and II in Fig. 2; the real $N_c = 3$ world has a $\sim$30% curvature correction), and hence both sides in the Clausius-Clayperon equation diverge. Percolation, however, implies a second-order phase transition; hence, the change in pressure [$P/(T\rho_B)$ jumps by $\sim N_c = 3$ when ρ_B crosses the percolation threshold, as quarks start exerting pressure] can only be *gradual* with density (the "jump" is a rapid but smooth crossover at any finite N_c), and there is no mixed phase or jump in energy density or heat capacity [$e/(T\rho_B)$ stays approximately constant as ρ_B is varied]. It would be very interesting to assess the effect of an equation of state with such a transition in calculations such as in Refs. [75,76,103–105].

In conclusion, we have studied the interplay between percolation and deconfinement in Yang-Mills matter at finite number of colors, temperature, and density. We find that these transitions exhibit a nontrivial dependence on N_c, suggesting that, at least for thermodynamics, we cannot automatically assume QCD is in the "large-N_c limit" at T, $\mu_Q \sim \Lambda_{QCD}$. Our calculations, however, show that the percolating phase *could* appear for $\rho_B \sim (0.125$–$3)\Lambda_{QCD}^3$, provided quarks at this density are still confined. Naive scaling in number of colors and flavors suggests they are, although we cannot say this with certainty. We have speculated what the dynamics of the percolating phase looks like and how it is related to popular approaches (such as the gauge/string duality) for describing Yang-Mills matter in the same regime. Even if the findings here will not be confirmed experimentally, characterizing them more rigorously on the lattice and in the gauge/string correspondence opens quite a few questions, the solutions of which could help us clarify the qualitative structure of Yang-Mills theories. Because a contact with our $N_c = 3$ world cannot be excluded, we have closed by suggesting experimental and astrophysical signatures of the percolating phase.

---

[5]We would like to thank Irina Sagert for discussions regarding this topic.

[1] G. 't Hooft, Nucl. Phys. B **72**, 461 (1974).
[2] E. Witten, Nucl. Phys. B **160**, 57 (1979).
[3] J. M. Maldacena, Adv. Theor. Math. Phys. **2**, 231 (1998); E. Witten, *ibid*. **2**, 253 (1998); S. S. Gubser, I. R. Klebanov, and A. M. Polyakov, Phys. Lett. B **428**, 105 (1998); J. M. Maldacena, arXiv:hep-th/0309246.
[4] A. V. Manohar, arXiv:hep-ph/9802419.
[5] L. Susskind, Phys. Rev. D **20**, 2610 (1979).
[6] L. D. McLerran and B. Svetitsky, Phys. Lett. B **98**, 195 (1981).
[7] J. Greensite, Lect. Notes Phys. **821**, 1 (2011).
[8] S. Borsanyi, Z. Fodor, C. Hoelbling, S. D. Katz, S. Krieg, C. Ratti and K. K. Szabo (Wuppertal-Budapest Collaboration), J. High Energy Phys. 09 (2010) 073.
[9] A. Bazavov *et al*., Phys. Rev. D **80**, 014504 (2009).
[10] I. R. Klebanov, Nucl. Phys. B **262**, 133 (1985).
[11] P. Danielewicz, R. Lacey, and W. G. Lynch, Science **298**, 1592 (2002).
[12] A. L. Goodman, J. I. Kapusta, and A. Z. Mekjian, Phys. Rev. C **30**, 851 (1984).
[13] M. D'Agostino *et al*., Phys. Lett. B **473**, 219 (2000).
[14] K. A. Bugaev, M. I. Gorenstein, I. N. Mishustin, and W. Greiner, Phys. Rev. C **62**, 044320 (2000).
[15] S. Das Gupta, A. Z. Mekjian and M. B. Tsang, arXiv:nucl-th/0009033.
[16] J. Pochodzalla *et al*., Phys. Rev. Lett. **75**, 1040 (1995).
[17] J. Gosset, H. H. Gutbrod, W. G. Meyer, A. M. Poskanzer, A. Sandoval, R. Stock, and G. D. Westfall, Phys. Rev. C **16**, 629 (1977).
[18] J. B. Elliott *et al*. (ISiS Collaboration), Phys. Rev. Lett. **88**, 042701 (2002).
[19] P. de Forcrand and M. Fromm, Phys. Rev. Lett. **104**, 112005 (2010).
[20] G. Torrieri and I. Mishustin, Phys. Rev. C **82**, 055202 (2010).
[21] S. Lottini and G. Torrieri, Phys. Rev. Lett. **107**, 152301 (2011).
[22] G. Torrieri, S. Lottini, I. Mishustin, and P. Nicolini, Acta Phys. Polon. Supp. **5**, 897 (2012).
[23] A. Mykkanen, M. Panero, and K. Rummukainen, J. High Energy Phys. 05 (2012) 069.
[24] M. Panero, Phys. Rev. Lett. **103**, 232001 (2009).
[25] O. Bergman, G. Lifschytz, and M. Lippert, J. High Energy Phys. 11 (2007) 056.
[26] M. Rozali, H. H. Shieh, M. Van Raamsdonk, and J. Wu, J. High Energy Phys. 01 (2008) 053.
[27] Z. Fodor and S. D. Katz, Phys. Lett. B **534**, 87 (2002).
[28] C. R. Allton, M. Doring, S. Ejiri, S. J. Hands, O. Kaczmarek, F. Karsch, E. Laermann, and K. Redlich, Phys. Rev. D **71**, 054508 (2005).
[29] P. de Forcrand and O. Philipsen, Nucl. Phys. B **642**, 290 (2002).
[30] P. Nicolini and G. Torrieri, J. High Energy Phys. 08 (2011) 097.
[31] G. Baym, Physica A **96**, 131 (1979).
[32] T. Celik, F. Karsch, and H. Satz, Phys. Lett. B **97**, 128 (1980).
[33] H. Satz, arXiv:hep-ph/0212046.
[34] F. Gliozzi, S. Lottini, M. Panero, and A. Rago, Nucl. Phys. B **719**, 255 (2005).
[35] L. McLerran and R. D. Pisarski, Nucl. Phys. A **796**, 83 (2007).
[36] T. Kojo, Nucl. Phys. A **877**, 70 (2012).
[37] L. Y. Glozman, V. K. Sazonov, and R. F. Wagenbrunn, Acta Phys. Polon. Supp. **5**, 717 (2012).
[38] S. Hands, S. Kim, and J. I. Skullerud, Phys. Rev. D **81**, 091502 (2010).
[39] A. Andronic *et al*., Nucl. Phys. A **837**, 65 (2010).

[40] L. McLerran, K. Redlich, and C. Sasaki, Nucl. Phys. A **824**, 86 (2009).
[41] K. Miura, T. Z. Nakano, and A. Ohnishi, Prog. Theor. Phys. **122**, 1045 (2009).
[42] M. Gazdzicki (NA61/SHINE Collaboration), J. Phys. G **36**, 064039 (2009); arXiv:0812.4415 [nucl-ex].
[43] A. N. Sissakian and A. S. Sorin (NICA Collaboration), J. Phys. G **36**, 064069 (2009).
[44] G. Odyniec, Acta Phys. Pol. B **40**, 1237 (2009).
[45] P. Staszel (CBM Collaboration), Acta Phys. Pol. B **41**, 341 (2010).
[46] G. Martens, C. Greiner, S. Leupold, and U. Mosel, Phys. Rev. D **70**, 116010 (2004).
[47] G. Martens, C. Greiner, S. Leupold, and U. Mosel, Phys. Rev. D **73**, 096004 (2006).
[48] G. Torrieri and S. Lottini, J. Phys. Conf. Ser. **426**, 012003 (2013).
[49] C. E. DeTar and J. F. Donoghue, Ann. Rev. Nucl. Part. Sci. **33**, 235 (1983).
[50] K. G. Wilson, Phys. Rev. D **10**, 2445 (1974).
[51] R. P. Feynman, Nucl. Phys. B **188**, 479 (1981).
[52] J. B. Kogut and L. Susskind, Phys. Rev. D **9**, 3501 (1974).
[53] M. Alford and K. Rajagopal, J. High Energy Phys. 06 (2002) 031.
[54] D. D. Dietrich and D. H. Rischke, Prog. Part. Nucl. Phys. **53**, 305 (2004).
[55] H. Abuki and T. Brauner, Phys. Rev. D **85**, 116004 (2012).
[56] A. Gerhold and A. Rebhan, Phys. Rev. D **68**, 011502 (2003).
[57] J. Rafelski, Acta Phys. Pol. B **43**, 829 (2012).
[58] J. Letessier and J. Rafelski, Camb. Monogr. Part. Phys. Nucl. Phys. Cosmol. **18**, 1 (2002).
[59] C. D. Lorenz, R. May, and R. M. Ziff, J. Stat. Phys. **98**, 961 (2000); C. D. Lorenz and R. M. Ziff, Phys. Rev. E **57**, 230 (1998).
[60] G. E. Brown, L. Grandchamp, C.-H. Lee, and M. Rho, Phys. Rep. **391**, 353 (2004).
[61] A. Heinz, F. Giacosa, and D. H. Rischke, Phys. Rev. D **85**, 056005 (2012).
[62] V. N. Gribov, Nucl. Phys. B **139**, 1 (1978).
[63] D. Zwanziger, Nucl. Phys. B **209**, 336 (1982).
[64] T. Kojo, Y. Hidaka, L. McLerran, and R. D. Pisarski, Nucl. Phys. A **843**, 37 (2010).
[65] T. Kojo, Y. Hidaka, K. Fukushima, L. McLerran, and R. D. Pisarski, Nucl. Phys. A **875**, 94 (2012).
[66] D. Stauffer and A. Aharony, *Introduction to Percolation Theory*, 2nd ed. (Taylor & Francis, London, 1991).
[67] J. C. Gimel, T. Nicolai, and D. Durand, J. Phys. A: Math. Gen. **32**, L515 (1999).
[68] R. Dekayser, Physica **31**, 1405 (1965).
[69] V. L. Bonch-Bruevich and V. B. Glasko, Opt. Spectrosc. [USSR; English translation] **14**, 264 (1963).
[70] G. Torrieri, arXiv:nucl-th/0405026.
[71] G. Torrieri and S. Vogel, Phys. Rev. Lett. **111**, 012301 (2013).
[72] P. Adhikari, T. D. Cohen, A. Jamgochian, and N. Kumar, Phys. Rev. C **87**, 035205 (2013).
[73] T. D. Cohen and V. Krejcirik, Phys. Rev. C **85**, 035205 (2012).
[74] R. F. Dashen, E. E. Jenkins, and A. V. Manohar, Phys. Rev. D **51**, 3697 (1995).
[75] T. Fischer, I. Sagert, G. Pagliara, M. Hempel, J. Schaffner-Bielich, T. Rauscher, F. K. Thielemann and R. Kappeli *et al*., Astrophys. J. Suppl. **194**, 39 (2011).

[76] I. Sagert *et al.*, Phys. Rev. Lett. **102**, 081101 (2009).

[77] See, for example, A. A. Shashkin *et al.*, Phys. Rev. Lett. **73**, 3141 (1994); Yigal Meir, *ibid.* **83**, 3506 (1999); S. Adam, S. Cho, M. S. Fuhrer, and S. Das Sarma, *ibid.* **101**, 046404 (2008).

[78] S. Carignano, D. Nickel, and M. Buballa, Phys. Rev. D **82**, 054009 (2010).

[79] W. Broniowski, Acta Phys. Pol. B Proc. Suppl. **5**, 631 (2012).

[80] D. Miskowiec, PoS C **POD07**, 020 (2007).

[81] S. Tomonaga, Prog. Theor. Phys. **5**, 544 (1950).

[82] F. D. M. Haldane, J. Phys. C **14**, 2585 (1981).

[83] A. J. Niemi, AIP Conf. Proc. **806**, 114 (2006).

[84] L. D. Faddeev and A. J. Niemi, Nucl. Phys. B **776**, 38 (2007).

[85] J. Wess and B. Zumino, Phys. Lett. B **37**, 95 (1971).

[86] S. P. Novikov, Usp. Mat. Nauk **37**, 3 (1982).

[87] E. Witten, Commun. Math. Phys. **92**, 455 (1984).

[88] P. J. Steinhardt, Nucl. Phys. B **176**, 100 (1980).

[89] A. R. Zhitnitsky, Phys. Lett. B **165**, 405 (1985).

[90] L. L. Salcedo, S. Levit, and J. W. Negele, Nucl. Phys. B **361**, 585 (1991).

[91] E. Abdalla and M. C. B. Abdalla, Nucl. Phys. B **255**, 392 (1985).

[92] Y. Frishman and J. Sonnenschein, Nucl. Phys. B **294**, 801 (1987); Phys. Rep. **223**, 309 (1993).

[93] A. Armoni, Y. Frishman, and J. Sonnenschein, Nucl. Phys. B **596**, 459 (2001).

[94] D. Mateos, S. Matsuura, R. C. Myers, and R. M. Thomson, J. High Energy Phys. 11 (2007) 085.

[95] I. R. Klebanov and M. J. Strassler, J. High Energy Phys. 08 (2000) 052.

[96] M. Mia, F. Chen, K. Dasgupta, P. Franche, and S. Vaidya, Phys. Rev. D **86**, 086002 (2012).

[97] A. L. Efros and B. I. Shklovskii, J. Phys. C: Solid State Phys. **8**, L49 (1975).

[98] B. Schuetrumpf, M. A. Klatt, K. Iida, J. Maruhn, K. Mecke, and P.-G. Reinhard, Phys. Rev. C **87**, 055805 (2013).

[99] S. Damjanovic *et al.* (NA60 Collaboration), Nucl. Phys. A **783**, 327 (2007).

[100] A. Adare *et al.* (PHENIX Collaboration), Phys. Lett. B **670**, 313 (2009).

[101] P. Demorest, T. Pennucci, S. Ransom, M. Roberts, and J. Hessels, Nature (London) **467**, 1081 (2010).

[102] F. S. Kitaura, H.-T. Janka, and W. Hillebrandt, Astron. Astrophys. **450**, 345 (2006).

[103] K. Nakazato, K. Sumiyoshi, and S. Yamada, Phys. Rev. D **77**, 103006 (2008).

[104] M. Hempel, T. Fischer, J. Schaffner-Bielich, and M. Liebendorfer, Astrophys. J. **748**, 70 (2012).

[105] J. A. Pons, A. W. Steiner, M. Prakash, and J. M. Lattimer, Phys. Rev. Lett. **86**, 5223 (2001).